Transactions, SMiRT-24
BEXCO, Busan, Korea - August 20-25, 2017
Division II

EXPERIMENTAL RESULTS AND NUMERICAL ANALYSIS OF TESTS CONDUCTED ON LARGE ALLOY 600 CENTRE-CRACKED TENSION SPECIMENS

Patrick Le Delliou[1], Anna Dahl[1], Christophe Sonnefraud[1], Willy Vincent[2]

[1] Research & Development Engineer, Materials & Mechanics of Components Department, EDF/R&D, France
[2] Laboratory Technician, Materials & Mechanics of Components Department, EDF/R&D, France

ABSTRACT

Some components of the main primary circuit of PWR nuclear power plants contain nickel-base alloy 600 parts (steam generator (SG) tubes, steam generator partition plates, lower internal radial supports). It is well know that this alloy is prone to stress corrosion cracking in the primary water environment. In 2002, surface cracks were discovered for the first time in SG partition plates of EDF 900 MWe NPP. The integrity of the SG containing these cracks must be demonstrated for all operating conditions, including accidental conditions. Due to the high tensile consolidation rate and the high fracture toughness of alloy 600, this was proved using limit load analysis. However, for a thorough demonstration, an experimental program was launched at EDF/R&D to better understand the behaviour of cracks in this high fracture toughness material. Centre-Cracked Tension (CCT) specimens were selected for this experimental program, being closer to the industrial case than conventional CT specimens.

Two tests have been conducted at room temperature on large CCT specimens containing a semi-elliptical crack. The paper presents the design of the CCT tests, the material characterisation, the main results of the tests and their numerical interpretation.

NOMENCLATURE

a	Crack depth (depth at the centre of a semi-elliptical crack)
B	Specimen thickness
b	Remaining ligament
c	Half-length of a semi-elliptical crack
CCT	Centre-cracked tension specimen
CT	Compact tension specimen
E	Young's Modulus
J	J-integral
J_{el}	Elastic component of J-integral
J_{pl}	Plastic component of J-integral
P	Applied load
SENT	Single-edge-notched tension specimen
W	Specimen width
Δa	Crack extension
ν	Poisson's ratio

1 INTRODUCTION

Some components of the main primary circuit of PWR nuclear power plants contain nickel-base alloy 600 parts (steam generator (SG) tubes, steam generator partition plates, lower internal radial supports). It is well know that this alloy is prone to stress corrosion cracking in the primary water environment. In 2002, surface cracks were discovered for the first time in SG partition plates of EDF 900 MWe NPP [1, 2]. The integrity of the SG containing these cracks must be demonstrated for all operating conditions, including accidental

conditions. Due to the high tensile consolidation rate and the high fracture toughness of alloy 600, this was proved using limit load analysis. However, for a thorough demonstration, an experimental program was launched at EDF/R&D to better understand the behaviour of cracks in this high fracture toughness material. Centre-Cracked Tension (CCT) specimens with a semi-elliptical surface crack [3] were selected for this experimental program, being closer to the industrial case (elongated surface cracks) than conventional CT specimens.

The paper is divided into three parts. In the first part the standard material characterization is described, which includes tensile mechanical properties (stress-strain curves) and crack resistance curves determined according to [4]. In the second part, the experimental work on the CCT specimens is introduced and commented. The last part is dedicated to the assessment of the CCT specimen tests based on the J-Integral approach.

2 STANDARD MATERIAL CHARACTERIZATION

The experimental work consists of tests of three different specimen sets:

- Tests on standard tensile specimens were performed to obtain stress-strain curves, which are used in the finite element simulation of the tests,
- Tests on CT specimens (CT25 and CT60) were performed to obtain crack resistance curves and to investigate the influence of the specimen size on the shape of the J-R curve,
- Tests on SENT specimens were performed to investigate the influence of the specimen geometry on the J-R curve. These tests will not be presented here.

2.1 Origin of the material

All the specimens were machined in a 68 mm thick alloy 600 plate, coming from a batch of 10 plates of the same heat. Table 1 gives the chemical composition of the plates. The plates are hot-rolled, with a final heat treatment at 1000°C during about 1 hour, followed by a water cooling.

Table 1: Chemical composition of the plates from the heat n°164645.

	C	S	P	Si	Mn	Ni	Cr	Fe	Cu	Co	Al + Ti
STR 4103	≤ 0.10	≤ 0.010	≤ 0.015	≤ 0.50	≤ 1.00	≥ 72.00	≥ 14.00 ≤ 17.00	≥ 6.00 ≤ 10.00	≤ 0.50	-	≤ 0.60
Supplier	0.07	0.002	0.008	0.27	0.29	73.05	16.33	9.35	0.03	0.06	-
EDF	0.065	0.002	0.007	0.25	0.27	Bal.	16.4	9.3	0.03	0.063	0.35

Tensile tests have been conducted at room temperature by the supplier according to ASTM E8 standard. The results are given in Table 2 and compared with ASTM B 168-08 standard specifications for alloy 600 at the annealed state.

Table 2: Tensile characteristics at 20°C of the plates of the heat n°164645. Two values of elongation at rupture are provided, according to the base: on 50 mm (4 diameters) and on 5 diameters (62.5 mm).

	$R_{p0,2}$ (MPa)	R_m (MPa)	A/50 mm (%)	A/5D (%)
Spec. B168-08	≥ 250	≥ 550	≥ 30	-
Supplier	278 - 265	670 - 663	45 - 46	43 - 43

2.2 Tensile tests

Tensile tests have been conducted at room temperature on round tensile specimens sampled in the rolling direction of the plate. Five specimens have been tested, all taken close to the mid-thickness of the plate. The

results are given in Table 3. Fig. 1 shows the corresponding true stress-true strain curves. The scatter between the curves is low.

Table 3: Tensile characteristics at 20°C of the plates of the heat n°164645 in the rolling direction, close to the mid-thickness.

Spec. ID	Spec. type	$R_{p0,2}$ (MPa)	R_m (MPa)	A/5D (%)	Z (%)
1840-B1-6B	TC5	237	651	44	66
1840-B1-6C	TC5	240	663	45	64
1966-TC6-1	TC6	231	655	48	65
1966-TC6-2	TC6	227	654	47	67
1966-TC6-3	TC6	236	665	47	61

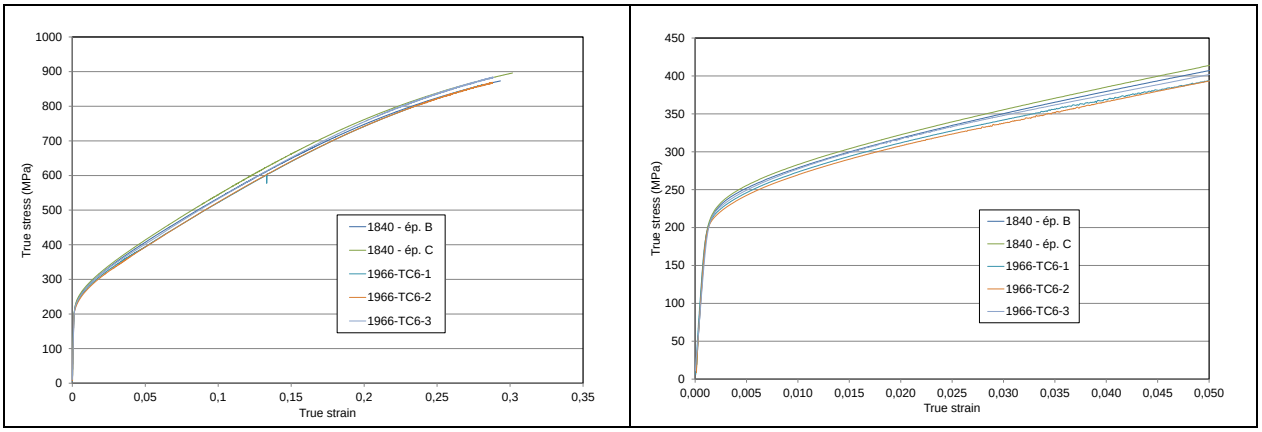

Figure 1: True stress-true strain curves at 20°C in the rolling direction of the plate.

2.3 Tests on CT specimens

Three sets of ductile tearing resistance tests have been conducted at 20°C on:

- CT25 specimens taken in the TL direction of the plate,
- CT60 specimens in the TL direction,
- CT25 specimens in the LS direction.

The large CT60 specimens allow to reach a large amount of crack growth (up to 7 mm), while the CT25 specimens in the LS direction are oriented like the CCT specimens that will be described further on. Table 4 summarizes the results obtained on the three sets of specimens. The J-R curves are fitted by a power law: $J = C\,\Delta a^n$. The J_{Ic} value is calculated with a blunting line slope equal to $4*\sigma_{flow}$, where σ_{flow} is the flow stress of the material (about 450 MPa). It should be noted that in the ASTM E 1820 standard [4], the slope is set to $2*\sigma_{flow}$, giving higher J_{Ic} values. Each test was conducted according to the single-specimen technique with periodic unloads, but was stopped after a selected displacement level, so the multiple-specimen technique can also been applied, by testing 4 or 5 specimens. The multiple-specimen technique tends to give lower J_{Ic} value than the single-specimen one. On the average, the J_{Ic} value is close to 600 kJ/m^2. Fig. 2 shows the single-specimen J-R curves for the CT60 specimens, whereas Fig. 3 shows the multiple-specimen J-R curve obtained with both CT60 and CT25 specimens taken in the TL direction.

Table 4: Ductile tearing resistance properties at 20°C of the plates.

Spec. Type/orientation	Technique	$J_{0.2} = J_{Ic}$ (kJ/m^2)	$J_1 = C$ (kJ/m^2)	n
CT25 - TL	Multiple-specimen	544	829	0.6174
CT60 - TL	Single-specimen	695	953	0.599
	Multiple-specimen	578	866	0.626
CT25 - LS	Multiple-specimen	613	847	0.524

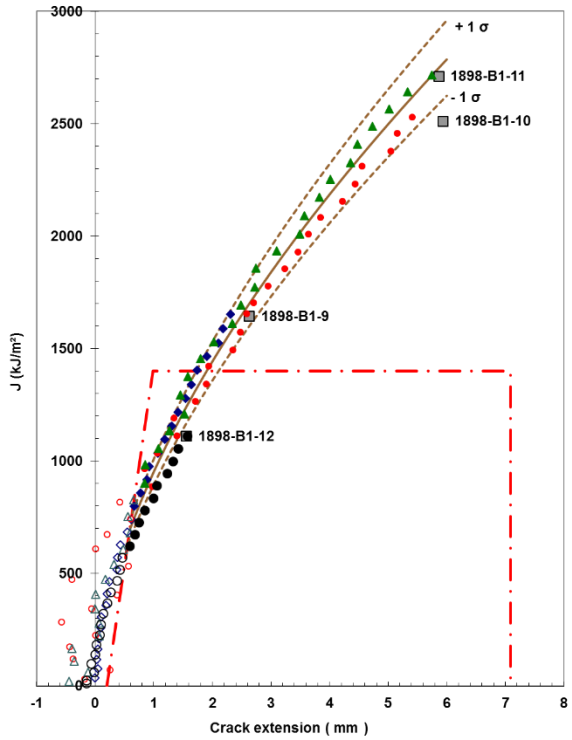

Figure 2: J-R curves for the CT60 specimens tested at room temperature (TL direction)

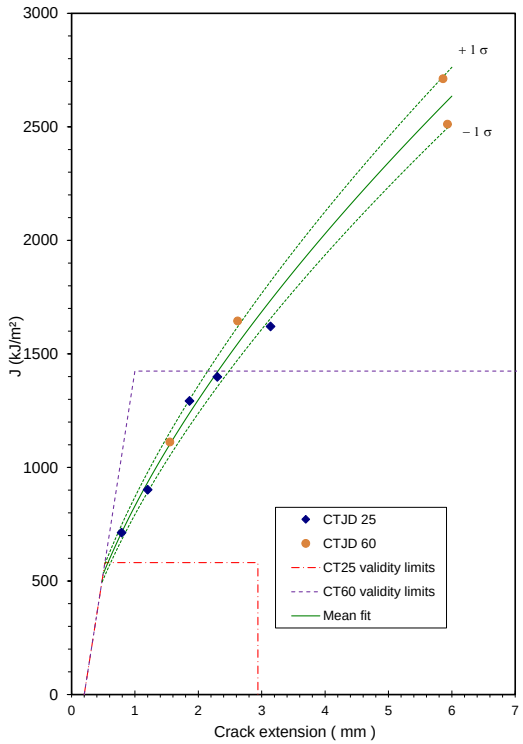

Figure 3: Multiple-specimen J-R curve for the CT60 and CT25 specimens tested at room temperature (TL direction)

3 EXPERIMENTAL WORK ON THE CCT SPECIMENS

Centre-Cracked Tension (CCT) specimens with a semi-elliptical surface crack [3] were selected because they are closer to the industrial case (elongated surface cracks in the SG partition plate) than conventional CT specimens.

3.1 Design of the specimens

A Centre-Cracked Tension specimen with a semi-elliptical crack perpendicular to the loading direction was designed. Fig. 4 shows the geometry of this specimen. The section of the central part of the specimen containing the notch equal 100x34 mm^2, whereas the heads containing the pin holes are reinforced, with a section equal to 174x60 mm^2. The purpose of the reinforcement is to limit the deformation of the heads and the holes during the test. Two tests were conducted, with two different crack sizes. The first test was dedicated to the crack initiation phase, whereas the second was designed to go up to the complete break of the specimen.

At the design stage, elastic-plastic finite element computations were conducted with various crack sizes (defined by a and c values) in order to select the most suitable crack size.

The notches were made by electric-discharge-machining, including integral knife edges to set the clip-gage. Prior to the ductile tearing test, each specimen was subjected to fatigue loading in tension in order to get a sharp crack front. Table 5 gives the sizes of the notch and of the crack for both specimens.

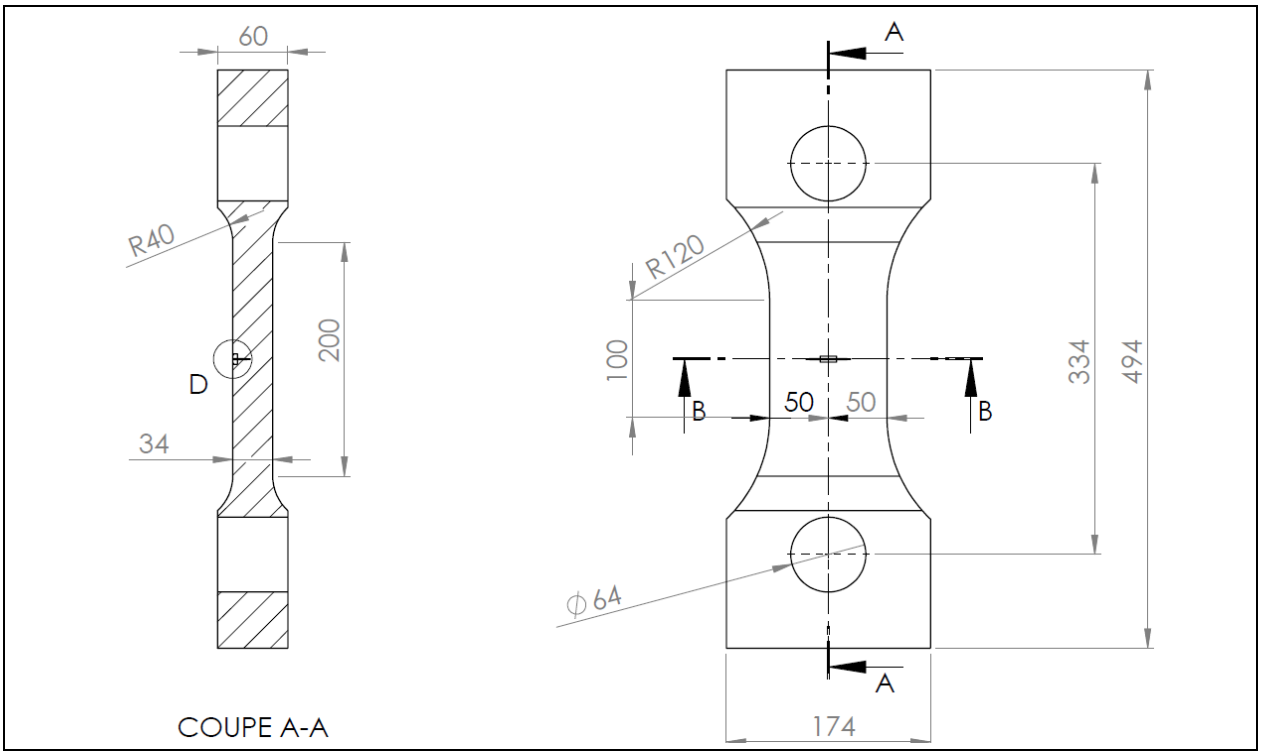

Figure 4: Geometry of the CCT specimen

Table 5: Notch size and crack size for the CCT specimens.

	Semi-elliptical notch		Semi-elliptical crack	
Specimen ID	a (mm)	c (mm)	a (mm)	c (mm)
CCT-1	15	19	17.5	21
CCT-2	22	29	24	33

3.2 Main experimental results

Fig. 5 and Fig. 6 compare respectively the load versus crosshead displacement curves and the load versus CMOD curves for the two tests. Partial unloads were done during both tests, and for the second test, a complete unload was done just after the maximum load was reached. During this particular unload, a fatigue cycling loading was applied to mark the crack front. The electric potential method was used during the tests to detect the ductile crack initiation and to follow the crack propagation. A constant d-c current was injected at 50 mm above and below the crack plane and the electric potential drop was measured at 5 points along the crack front (centre, both crack tips and at mid distance between the centre and the crack tips). Fig. 7 and Fig. 8 show the evolution of the ep drop at the crack centre as a function of the CMOD for each test. The crack initiation corresponds to the point where the curve starts to deviate from the tangent line. Before this point, the ep drop increase is attributed to geometry changes in the specimen.

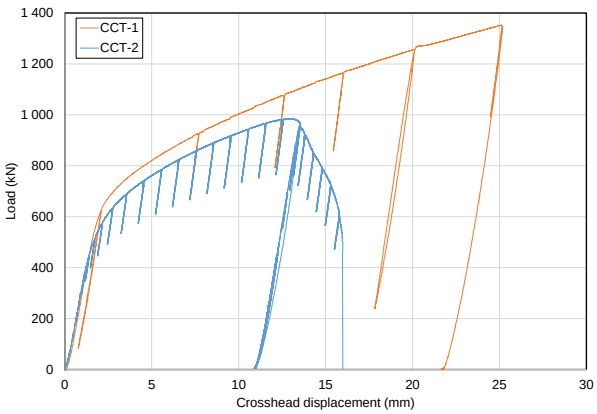

Figure 5: Comparison of the load versus vs crosshead displacement curves for the CCT tests

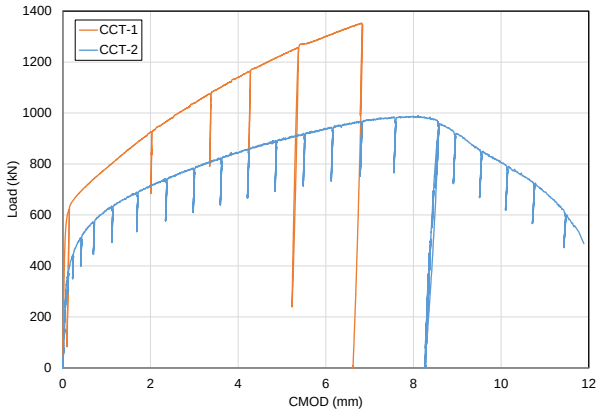

Figure 6: Comparison of the load versus CMOD curves for the CTT tests

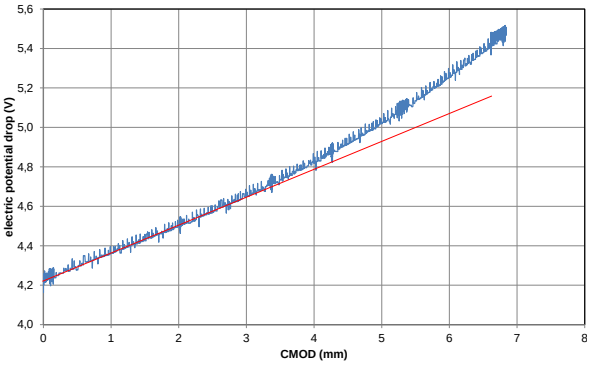

Figure 7: Determination of the crack initiation CMOD for the CCT-1 test

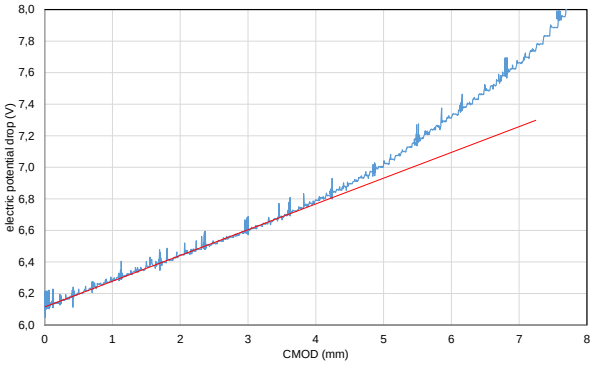

Figure 8: Determination for the crack initiation CMOD for the CCT-2 test

Fig. 9 shows the central part of the CCT-1 specimen at the end of the test. On this picture, one can see the d-c current injection points, the wires to measure the electric potential drop, and the white paint with black dots used for the digital image correlation method. After the test, the specimen was heat tinted and then fatigue post-cracked in tension in order to break it completely without introducing additional deformations. Fig. 10 shows the fracture surface of the CCT-1 specimen. The red arrows identify the different zones of the fracture surface: machined notch, fatigue pre-cracking, ductile tearing, fatigue post-cracking and final rupture of the remaining ligaments. At the deepest point of the defect, the ductile tearing is close to 3 mm.

Fig. 11 shows the central part of the CCT-2 specimen at the end of the test, i.e. the final unload on Fig. 5 (this rapid unload triggered the hydraulic machine). This unload corresponds to the failure of the ligament situated on the right side of the picture. The remaining ligament, on the left side of the picture, was broken by fatigue post-cracking in tension. Fig. 12 shows the fracture surface of the CCT-2 specimen. The red arrows identify the different zones of the fracture surface: machined notch, fatigue pre-cracking, ductile tearing, and fatigue post-cracking of the remaining ligament. On this specimen, the ductile tearing is first flat before evolving towards a slant rupture. Fatigue post-cracking was used to break the small ligament at the left side of the picture. The very tiny white line visible on the picture is the beach-mark done by the fatigue cycling loading applied just after the maximum load.

Figure 9: View of the central part of the CCT-1 specimen at the end of the test

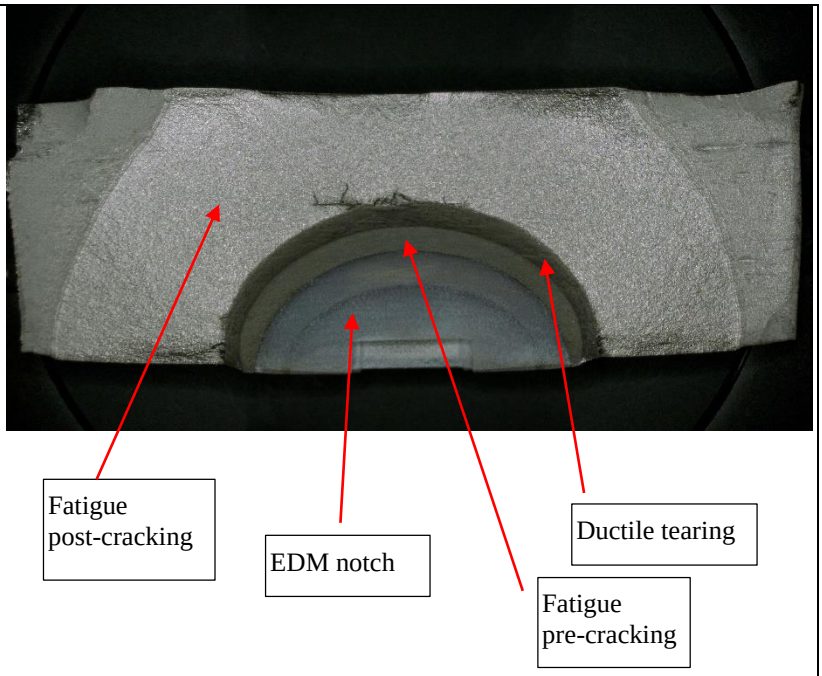

Figure 10: View of the fracture surface of the CCT-1 specimen

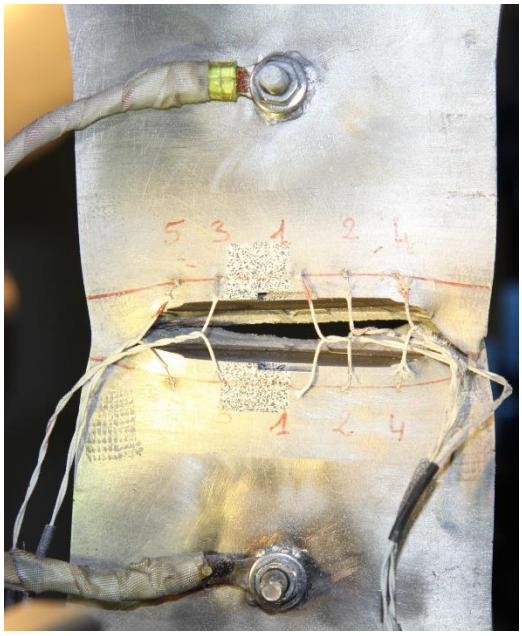

Figure 11: View of the central part of the CCT-2 specimen at the end of the test

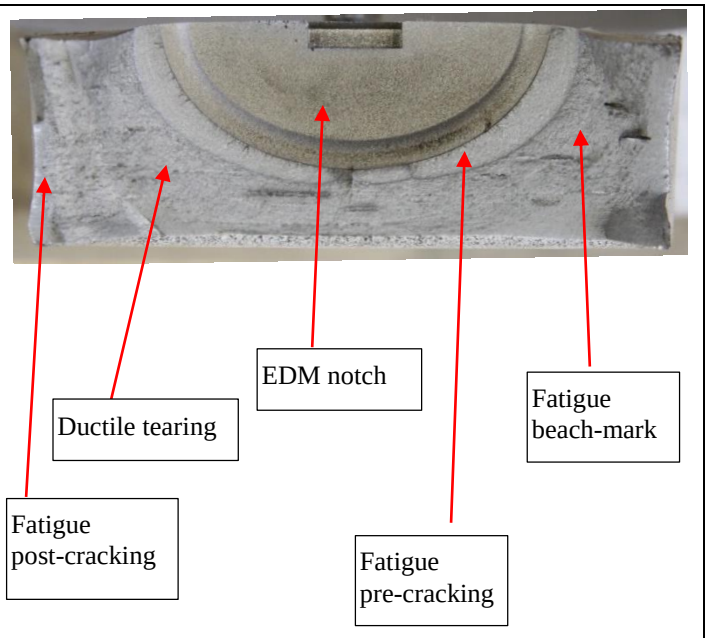

Figure 12: View of the fracture surface of the CCT-2 specimen

4 NUMERICAL ANALYSIS OF THE CCT TESTS

4.1 Principle of the numerical analyses

For the first test and for the second test up to the total unload, the ductile crack extension is limited to few millimetres and the crack shape remains approximately semi-elliptical. A conventional J-integral analysis based on a J-Δa diagram is used. To use this approach, several finite element computations are conducted with different crack sizes and the J-integral is computed. The J-integral values are extracted for different crack sizes under constant load (here for example under 1050, 1100… 1370 kN, see Fig. 16). These "applied J" curves and the material J-R curve are plotted on a J-Δa diagram. Using this diagram, one can predict the crack extension for a given load and the onset of the instable propagation, when the J-R curve becomes tangent to an "applied J" curve.

For the second test after the total unload, the ductile crack extension is large, the crack shape is no longer semi-elliptical, and after a certain point, the ductile tearing moves towards the slant mode (shear tearing). The crack extension can be simulated by the node-release technique, but this technique needs to know the evolution of the crack extension as a function of the loading parameter and therefore it is not predictive. A more advanced approach based on micromechanical models such as the Gurson's model or the Rousselier's model can predict the crack extension, at least in the "flat" mode stage. Predict the change to the slant mode is more challenging.

4.2 Analysis of the first test

Taking into account the symmetries, only one-quarter of the specimen is modeled. Three models were assessed: with only a part of the pin (Fig. 13), with the pin, and with the pin and the clevis (Fig. 14). With this more complicated model, contact conditions must be applied. It appeared that the three models gave about the same load versus CMOD curves, so the simplest one was kept for the study.

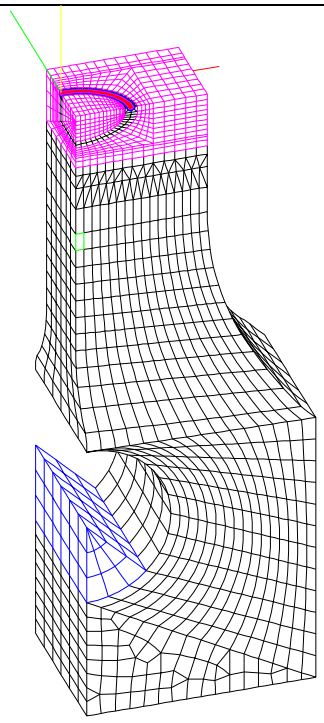

Figure 13: Example of a mesh with a semi-elliptical crack a = 17 mm and c = 21 mm

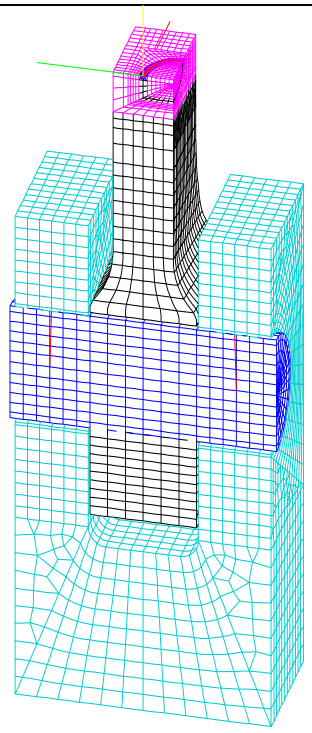

Figure 14: Example of a mesh with a semi-elliptical crack a = 17 mm and c = 21 mm

Besides the initial crack size (a x c = 18 x 21 mm^2) and the final crack size (a x c = 20.9 x 22.75 mm^2), four intermediate crack sizes were selected for the analysis of the crack propagation. Fig. 15 shows the load versus CMOD curves corresponding to these different cracks, compared with the experimental curve. Fig. 16 shows the analysis of the crack propagation. Both the crack initiation and the final crack extension are well predicted.

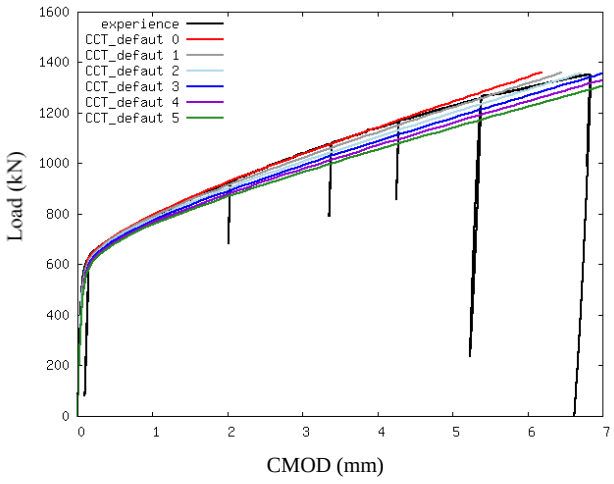

Figure 15: Load versus CMOD curves for the different crack sizes. The black curve corresponds to the experimental one

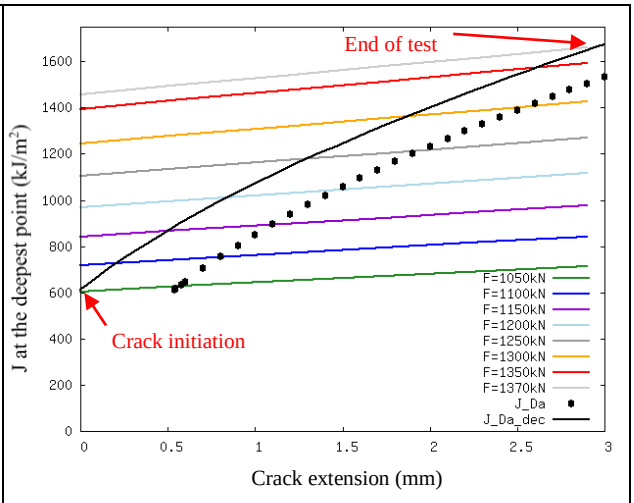

Figure 16: J-Δa diagram showing the analysis of the crack propagation

4.3 Analysis of the second test

Up to the total unload where the crack extension is limited to few millimetres and the crack shape stays semi-elliptical, the conventional J-integral analysis applied to the first test was used. This approach was used at the design stage and appeared rather accurate up to the maximum load, as shown on Fig. 17. After this point, the shape of the crack starts to departure from the semi-elliptical one. The same approach was used for the post-test assessment, based on the measured crack shapes (Fig. 12). After the maximum load, the node-release technique was used to derive the load versus CMOD curve. This technique gives good results but is not predictive. Work is underway to apply a more advanced methodology, based on micromechanical models.

5 CONCLUSIONS

A large experimental program was conducted to better understand the ductile crack propagation in industrial structures made of nickel-base alloy 600. Besides tests on conventional laboratory specimens, two tests were conducted on large CCT specimens containing a semi-elliptical crack. The first test was stopped after a limited amount of ductile tearing, whereas the second was carried out up to the fracture of the specimen.

The conventional J-integral analysis gives good results as long as the crack extension is limited to few millimetres, but that is enough to predict the maximum load. To go further, the node-release technique provides the load versus CMOD curve, but it requires as an input the evolution of the crack extension, so it is not predictive. The micromechanical models like the Gurson's model are able to predict the crack extension, at least as long as the crack stays in its initial plane.

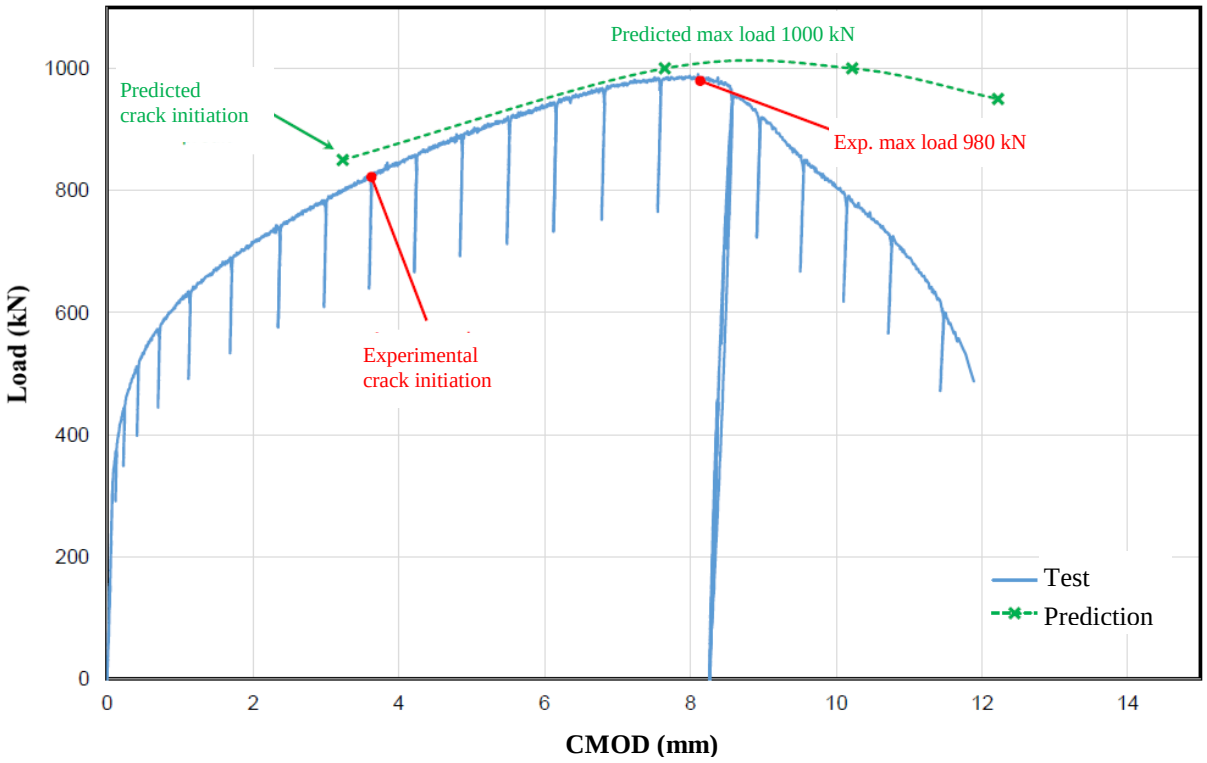

Figure 17: Load versus CMOD curve for the CCT-2 specimen. Comparison between the predicted curve and the experimental one

6 REFERENCES

[1] Bibollet, C. et al, 2006, "EDF field experience on steam generator divider plate examinations", *Proceedings Fontevraud 6 International Symposium, Contribution on material examination to the resolution of problems encountered in PWR*, SFEN

[2] Rossillon, F., Depradeux, L., Miloudi, S. et al, 2011, "Learnings from investigations on SG divider plates: coupling field characterizations with numerical mechanical simulations", *Proceedings SMIRT 21 Conference*, paper ID# 406

[3] Nicak, T., Schendzielorz, H., and Keim, E., 2009, "Analysis of fracture mechanics specimens made of Inconel 600 based on assessment methods of different complexity", *Proceedings of ASME 2009 PVP Division Conference*, paper PVP2009-77195

[4] ASTM E 1820-11 (2011). "Standard test method for measurement of fracture toughness", *American Society of Mechanical Engineers*